Effect of disorderness in two-dimensional discrete adiabatic combustion waves in a heterogeneous solid medium under stable regime

Naine Tarun Bharat* and Debi Prasad Mishra
Combustion Laboratory, Department of Aerospace Engineering, Indian Institute of Technology Kanpur, Kanpur 208016, India

(Received 14 February 2019; revised manuscript received 18 April 2019; published 13 June 2019)

The effect of disorderness for the propagation of stable combustion waves in a two-dimensional discrete adiabatic system are studied by considering two systems, namely, (i) periodic and (ii) disorder. The discrete periodic system is modeled by regular arrangement of burnt and unburnt point heat sources. In contrast, the discrete disordered system is modeled by the concatenation of regular burnt and randomly distributed unburnt heat sources. Four different kinds of discrete disordered systems (S1, S2, S3, and S4) are modeled by varying the joint frequency count of unburnt heat sources without changing the domain size of the system. Results show that the disordered structure of the discrete system plays a crucial role in the combustion dynamics, shape of the combustion wave, and it affects the propagation of stable combustion waves with the manifestation of sparse and chaotic finger patterns. Quantitative analysis performed for the width and roughness of combustion front show that the disordered structure and ignition temperature (ε) of the discrete system plays a crucial role. The burn rates of discrete system are sensitive to change in structure of the system and ε. It is observed that the burn rates obtained for the discrete disordered system is always less than that of burn rates of the discrete periodic system. The burn rates calculated for the present model are compared with the available experimental data on combustion of thermite systems.

DOI: 10.1103/PhysRevE.99.062114

I. INTRODUCTION

Heterogenous combustion can be observed in burning of solid propellants [1–8], composite modified double base propellants [7,8], burning of powder mixtures [5], etc. Powder mixtures are the simplest form of heterogenous systems in which the combustion occurs without notable gasification [1–8], and the reactants change their chemical state immediately after their melting point. Hence, such heterogenous systems are realized as gasless combustion. Burning of solid propellants [6–8], thermite mixtures [5], and powder reactants such as Ti + xSi, Ta + xC [1–8], the self-sustained combustion can be realized only within the concentration limits of mixtures.

Heterogeneous combustion consists of one or more reactants that undergo chemical change near the region of glowing combustion front [1–6]. Heterogenous systems with different binders, stoichiometry coefficient, or different diluter have different burning temperatures and burn rates [5]. Experimental studies [5–15] on combustion of such heterogenous systems, using high-speed microvideo recorder, have revealed that at microtimescale the combustion wave (front) becomes more complex and can be represented as random burning of hot spots. The combustion wave in heterogenous systems propagates with micro-oscillations even in stable mode. These micro-oscillations of combustion wave lead to combustion instabilities [9–11]. As a consequence, the combustion front in the reaction region starts propagating slowly with emission of products which do not glow in visible light. These observations suggest that the dynamics of combustion wave are localized to the vicinity of reactants interaction. And they indicate that the change of binder or diluter or stoichiometry during the preparation of heterogenous systems automatically forms the internal microstructure and consequently effect the dynamics of combustion process. Ory Zik *et al.* detected the combustion instabilities and finger patterns, during their experimental works [9–11], when a solid fuel is forced to burn against the oxidizing wind. Fingers and space in finger patterns in combustion front were related to the reactant transport and heat loss. Previous experimental work [9–15] show that the heat loss plays a crucial role in the occurrence and development of fingering instability. Analysis of combustion front patterns and instabilities were limited to experimental investigations [2–15] till now. In addition to that, the experimental research is too expensive and requires safety measures. Difficulties and uncertainties often associated with experimental determination of combustion instabilities [1–15] are overcome by mathematical modeling and numerical simulation. Hence theoretical models and computer-based simulations are considered as an alternative method of estimating the combustion behavior over wide ranges of operating conditions.

Recent theoretical studies have shown that the heterogenous systems are well represented and described by discrete combustion models [16–24]. Such theoretical works [16–19,22–24] on discrete combustion wave show the occurrence of kinetic roughening of combustion front. However, the role of disorderness in effecting the dynamics of combustion process at a particular ignition temperature is neglected. Internal structure which is *a priori* unknown plays an important role in deciding the dynamics of heterogenous combustion [16–19,22–24]. And the diagnosis of combustion wave with effect to change in disorderness is important and interesting.

*tarunbn@iitk.ac.in; nainetarun@gmail.com

There were very few works devoted to the mathematical modeling [16–19,22–24] and dynamical behavior of combustion front patterns [25–31]. In such situations the diagnosis of combustion wave is one of the most challenging areas. Mathematical modeling and numerical simulation of such combustion instabilities is of fundamental importance and study in these directions can provide solutions to understand the various physical parameters of heterogenous combustion, such as modes of combustion, flame structure, and burn rates. Hence, the role of internal structure of heterogeneous system cannot be neglected.

The model of discrete combustion waves [16–19,22–24,33–39], which has a very interesting behavior, similar to the behavior of the combustion of actual heterogeneous systems, has been considered here. The present work investigates for the effect of change in internal structure on reaction rate, flame structure, and combustion instabilities in two-dimensional discrete periodic and random (disordered) system. Arrangement of burnt and unburnt cells on a two-dimensional plane is done in periodic and disordered manner. This method of modeling the combustion process requires dedicated huge computing source for a couple of months. In addition, the computation load increases with increase in size of domain, randomness, and periodic boundaries of discrete system. Consequently, simulation of a two-dimensional combustion process requires high-performance parallel computing. Desktop systems with single processor takes nearly 1–2 months for numerous loop iterations. However, the advancements in high-performance parallel computing with message-passing interface (MPI) programming paved a path to access the nodes simultaneously. MPI provides widely used standards for writing message-passing programs. MPI programming is apt for numerical simulations, since it provides task parallelism along with data broadcasting and data gathering in synchronization. The ability to utilize MPI programming to achieve fast and accurate computation of combustion process allows for efficient and reliable analysis on calculated data. Implementation of modeling and numerical simulation of combustion process is discussed in the present work in the context of optimized computing time, ignition time profile, reaction rates, and structure of combustion front. The diagnosis of rate of combustion front (rate of thermal fluctuations) enhances the fundamentals of combustion kinetics and aids in improving the performance of those engineering devices that utilize it.

II. MODELING

The two-dimensional discrete combustion model is based on the existing theories of flame propagation, which assumes the width of the heating and reaction zones are much greater than the size of individual powder particles [16–21,32–38]. Propagation of combustion front is modeled by distributing combustible point heat sources (burnt and unburnt cells) in ordered, random methods as shown in Secs. IIIB and IIIC1. Initial burnt cells at time $t = 0$ allows for the self-sustained propagation of combustion front. And it is assumed that the spontaneous ignition and burning away of the unburnt particle occurs as soon as the temperature reaches a predetermined ignition temperature ($T_{\rm ign}$). Detailed description of the discrete system is seen in Secs. IIIB and IIIC1. Experimental data [1–6,14] show that the chemical reaction between the reactants starts practically immediately after the appearance of the liquid phase in the system and the burn-out time for the active particles is always essentially less (at least order) than the characteristic time of the heating of the particles from the initial temperature up to ignition temperature. This allows us to consider the process of the burn-out of the reaction cells of the system as instantaneous and the instant of reaching of some threshold temperature $T_{\rm ign}$, at which a liquid phase (e.g., molten materials or eutectic) appears in the system, can be considered as an instant of the ignition of the cells. Such a two-dimensional discrete system (shown in Figs. 2 and 5), consisting of the point heat sources (reaction cells), distributed along an axis (x, y), in ordered and uniform random distribution fashion, have been considered in the present work. The problem is explained by two-dimensional equation with δ sources given by

$$T[t, (x, y)] = T_{\rm in} + \sum_{i(t)} \Delta T_i\{t - t_i, [(x - x_i), ((y - y_i))]\}, \tag{1}$$

where $T_{\rm in}$ is the initial temperature of the system; t_i is the instant of ignition of the ith cell, located at $(x_i y_i)$ and $\Delta T_i(t, (x, y))$ is the temperature induced at the point (x, y) at time moment t by a single-point heat source, located at $(x, y) = 0$ and ignited at time moment $t = 0$.

For a two-dimensional problem the function $\Delta T_i[t, (x, y)]$ [16–19,32–38] in Eq. (1) with initial condition $T(x = 0, y = 0, t = 0) = mf(x)$, where $f(x) = 0$ for $x, y \neq 0$, $f(x) = 1$ for $x, y = 0$ and boundary conditions $T(x, t) \to 0$ for $x \to \pm\infty$ and $T(y, t) \to 0$ for $y \to \pm\infty$ is obtained as

$$\Delta T_i(t, (x, y)) = \left(\frac{Q_i}{c\rho}\right)\frac{1}{4\Pi\kappa \rm t}\exp\left(\frac{-(x^2 + y^2)}{4\kappa \rm t}\right), \tag{2}$$

by using the superposition of the Green's function for the diffusion equation [16–19,32–38]. The two-dimensional diffusion equation with source term [16–19,32–38] can be used for description of the evolution of the temperature of actual combustible system. And the temperature of heat source (x_k, y_k) at time t is given as

$$T(t, (x_k, y_k)) - T_{\rm in} = \frac{1}{4\Pi}\sum_{i=-\infty}^{m(t)}\sum_{j=-\infty}^{\infty}\frac{1}{(t_k - t_{(i,j)})} \times \exp\left(\frac{-((x_k - x_i)^2 + (y_k - y_i)^2)}{4(t_k - t_{(i,j)})}\right). \tag{3}$$

Here $i = -\infty \to m(t)$ is referred to as the arrangement of burnt and unburnt cells. Where $m(t)$ in Eq. (3) is the number of a last source ignited by time t. And $j = -\infty \to \infty$ is referred to as the periodic boundary condition along the y axis. The periodic boundary condition is introduced to exclude the influence of inflammation of the point heat sources of the discrete system under consideration. The ignition temperature

$T_{\rm ign}$ and specific heat cρ is considered as identical for all heat sources. In this case the reaction propagates consecutively from source to source, and a source (i,j) can be ignited only after ignition of the source $(i-1, j-1)$. At time t_k of the temperature of heat source $T[t,(x_k,y_k))]$ is now replaced by $T_{\rm ign}$ and the Eq. (3) is converted to

$$T_{\rm ign} - T_{\rm in} = \frac{1}{4\Pi}\sum_{i=-\infty}^{m(t)}\sum_{j=-\infty}^{\infty}\frac{1}{(t_k - t_{(i,j)})} \times \exp\left(\frac{-((x_k-x_i)^2+(y_k-y_i)^2)}{4(t_k-t_{(i,j)})}\right). \quad (4)$$

Now introducing dimensionless parameters, ignition time $t = t(\frac{k}{l^2_{(x,y)}})$ is the time required for each unburnt particle to reach the ignition temperature, location of nondimensional point heat sources $x_k = \frac{x}{l_x}$; $y_k = \frac{y}{l_y}$, nondimensional ignition temperature $\varepsilon = \frac{(T_{\rm ign}-T_{\rm in})}{(T_{\rm ad}-T_{\rm in})}$ is defined as the predetermined ignition temperature of the discrete system and $T_{\rm ad}$ is adiabatic temperature, $T_{\rm in}$ is initial temperature, $T_{\rm ign}$ is ignition temperature of system, and heat released for burnt particle denoted by $q_{i,j} = \frac{Q_{i,j}}{Q_o}$ is assumed to be unit, where $T_{\rm ad} = T_{\rm in} + (\frac{Q_{i,j}}{c\rho l_o})$ is mean adiabatic temperature of the thermal bridge, $Q_o = \lim_{N\to\infty}\frac{1}{N}\sum_{i=1}^{N} Q_{i,j}$ is a mean energy release in combustion of one heat source, and $l_x = \lim_{N\to\infty}(\frac{x_N-x_o}{N})$; $l_y = \lim_{N\to\infty}(\frac{y_N-y_o}{N})$ is a mean distance between neighbor point heat sources in the system. Equation (4) is the following:

$$4\Pi\varepsilon = \sum_{i=-\infty}^{k-1}\sum_{j=-\infty}^{\infty}\frac{q_{i,j}}{t_{k,j}-t_{i,j}} \times \exp\left(-\frac{(x_{k,j}-x_{i,j})^2+(y_{k,j}-y_{i,j})^2}{4(t_{k,j}-t_{i,j})}\right), \quad (5)$$

for given $t_i (i<k)$. Equation (5) is utilized for the numerical calculation of ignition times of unburnt heat sources in the discrete periodic and disordered systems. All the solutions of the discrete system depend on single parameter (ε).

Nondimensional burn rate (reaction rate) [32–38] of the two-dimensional discrete system is introduced as ω. Calculation of burn rates (ω) is crucial for the quantification of combustion front. The combustion of such developed system occurs nonuniformly in a pulsating mode (shown in results section), and because of this a mean burn rate is considered. Mean burn rate of combustible system is given by

$$\omega = \frac{\frac{(N_k-N_i)}{(t_k-t_i)}}{l_y}, \quad (6)$$

where N is number of burnt particles and t is ignition time. Note suffix k and i refer to later and former layer of reaction cells in case of an ordered system. l_y is the domain size of discrete system along the y axis. Numerical simulation of two-dimensional combustion is performed by governing Eqs. (5) and (6) in the Results section.

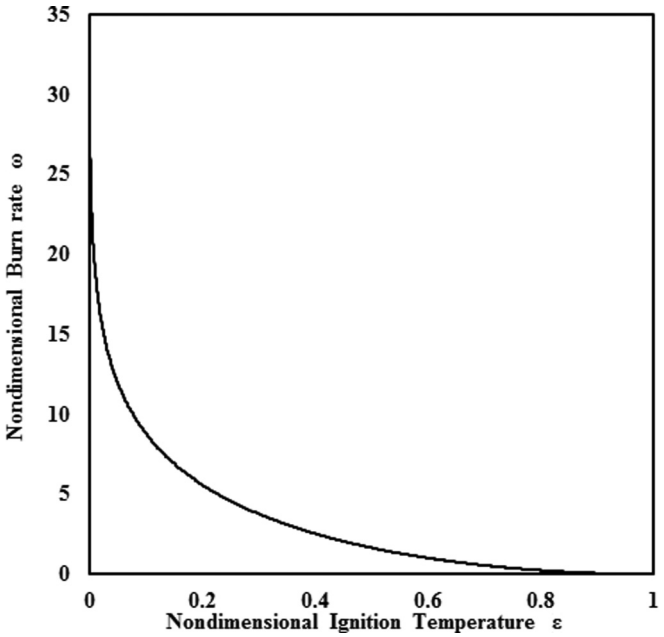

FIG. 1. Plot for nondimensional ignition temperature ε and burn rate ω.

III. RESULTS AND DISCUSSION

A. Theoretical analysis of the ideal system

The present section describes the ideal system [32–38], where the combustion front exists for all nondimensional ignition temperatures (ε) and propagates in steady state. Consider the two-dimensional ideal (continuum model) system with continuous point heat sources; that is, in the system under consideration $x_k = kl_x$, $y_k = kl_y$, and $Q_k = Q_{(x,y)}$ for all k. The ignition delay time or induction period (Δt) is introduced as time interval between two neighboring point heat sources and is given as

$$\Delta t = (t_k - t_i).$$

The quantity reciprocal to the induction period (Δt) can be considered as velocity of combustion front or burn rate (ω) over the length between the sources k and I,

$$\omega_{ki} = \frac{1}{\Delta t},$$

for all i. In this case, with $t_k = \Delta t * k$ then Eq. (5) becomes

$$\varepsilon = \omega^{\frac{1}{2}}\sum_{\rm i=1}^{\infty}\sum_{\rm j=-\infty}^{\infty}\frac{1}{(4\pi i)^{\frac{1}{2}}}\exp\left(-\frac{\omega}{4i}(i^2+j^2)\right), \quad (7)$$

where ω is burn rate, (i, j) represents position of combustion front, and ε is the ignition temperature. Solid line in Fig. 1 shows the plot for theoretical dependence $\omega(\varepsilon)$ using Eq. (7). Burn rate (ω) decreases with increase in nondimensional ignition temperature (ε). This observation for dependence ε-ω is similar to the experimental data [1–8,14]. Experimental works have shown that the ignition time and burn rate varies with change in diluter and amount of diluter [5–8,14]. It is observed from Fig. 1 that the theoretical solution for dependence $\omega(\varepsilon)$ exists for all values of $0 < \varepsilon \leqslant 1$.

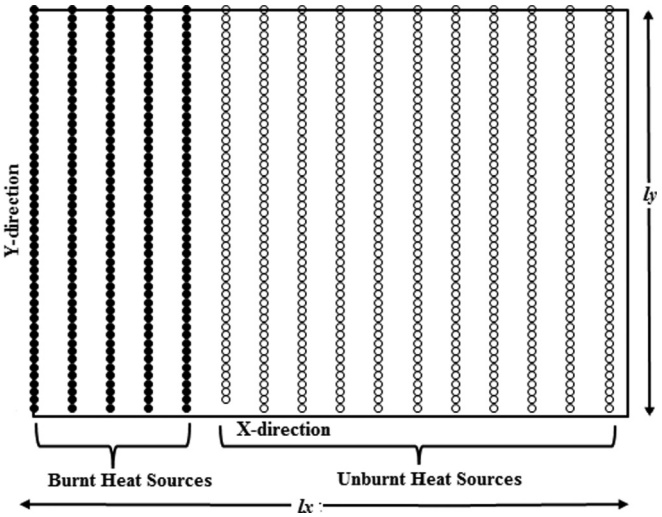

FIG. 2. Structure of a two-dimensional discrete periodic system. '●' represents the burnt particles and "o" is for unburnt particles.

Equation (7) used for the ideal system cannot explain the complex behavior of actual combustion process. The combustion dynamic parameters such as structure of combustion front and modes of combustion front cannot be predicted using the ideal system. However, the observations from the results of the ideal system are taken as reference for the numerical simulation of the discrete periodic system using Eqs. (5) and (6). In addition, this numerical exercise for the ideal system also facilitates in deciding the domain size of a two-dimensional discrete periodic system.

B. Discrete periodic system

1. Realization of discrete periodic system

A two-dimensional discrete periodic system, as shown in Fig. 2, consists of point heat sources distributed orderly along an axis x and y. l_x, l_y are the dimensions along x and y directions. The domain size of a two-dimensional discrete periodic system is 54×200, where $l_x = 54$ and $l_y = 200$. Total point heat sources (10 800) in the system are divided into two categories those are 4800 burnt sources (represented by '●') and 6000 unburnt sources (represented by '○'). Heat transfer between point source particles is carried through the thermal bridge and it is assumed that there is no heat loss; i.e., total heat energy released by combustion of burnt particle is totally utilized for combustion of succeeding unburnt particles [32–38].

A sufficient amount of thermal energy required for the initiation of propagation of combustion front is achieved by considering initial burnt particles at time $t = 0$. The point heat sources (cells) are considered to be immobile and are characterized by a nondimensional ignition temperature (ε). As soon as the temperature of an unburnt cell reaches the value of predetermined ignition temperature (ε), the ignition and instantaneous burning away of the cell occurs with the release of heat Q_i. The simulation of combustion process for the discrete periodic system is performed by Eq. (5). In the numerical simulations of two-dimensional combustion, the temperature changes arising due to inhomogeneity of the domain size of the discrete system affect the combustion process. Ignoring these temperature changes can cause unphysical dynamics while performing numerical simulation [16–19]. Incorporating periodic boundary can account for accurate physical dynamics [16–19]. Periodic boundary is taken as mirror image of reacting domain with coordinates (x_i, y_i) along upstream and downstream. The coordinates for mirror image with periodic boundary m are given as $(x_i, y_i \pm ml_x)$. The value of periodic boundary (m) [16–19] is decided from the knowledge of results obtained using Eq. (7). The discrete periodic system with domain size 54×200 and periodic boundary m is now computed using Eq. (5). The simulation of the discrete periodic system is performed as follows. Given predetermined ignition temperature (ε) discretize the two-dimensional combustible system with sufficient burnt cells [$ly\times$ (burnt-1)] and unburnt cells ($lx \times ly$). Note initial periodic boundary (m). At time $t = 0$ all the burnt cells are ignited. Time (t) is incremented by dt and the temperature of all the unburnt cells is calculated using Eq. (5). The temperatures of all unburnt cells are compared with the predetermined ignition temperature (ε). If the temperature of an unburnt cell is $\geqslant \varepsilon$, then it is transferred to burnt cells, else the time (t) is again incremented and calculation of temperatures are repeated. Calculation of temperature of unburn cells are repeated until all the unburnt cells are transferred to burnt cells. Using the times of ignition and Eq. (6), the burnt rate for the discrete periodic system is calculated. Calculations are repeated for each incremented value of periodic boundary condition until the critical periodic boundary is reached. Critical periodic boundary is referred to as the value of a parameter beyond which it does not affect the burn rate. And the above calculations are repeated for each value of predetermined ignition temperature (ε). Since the execution time using C code by desktop computer is of the order of multiple months for a single ignition temperature (ε), this hurdle is overcome by utilizing MPI programming. The discussion for the utilization of MPI technique and slice reconfiguration scheme for the simulation of combustion process is presented in the Appendices.

2. Results

The mathematical modeling and numerical simulation of a two-dimensional discrete periodic system has allowed obtaining ignition time profiles, flame structure and burn rate at different nondimensional ignition temperatures. Ignition time profiles of a discrete periodic system is shown in Fig. 3. Ignition time of unburnt heat source increase with increase in nondimensional ignition temperature (ε). And the steps in Fig. 3 indicate that the unburnt point heat sources are burnt layer by layer.

The structure of combustion front for the discrete periodic system at ignition temperature $(\varepsilon) = 0.4$ is shown in Fig. 4. The visualization of small domain of the discrete periodic system represented by dashed arrow which indicates the extension of Y axis till size 200. Combustion front in the discrete periodic system propagates layer by layer. All unburnt heat sources in layer are burnt at single time. This fashion of burning heat sources produces sufficient heat energy and ensures that the combustion is self-sustained and stable. And

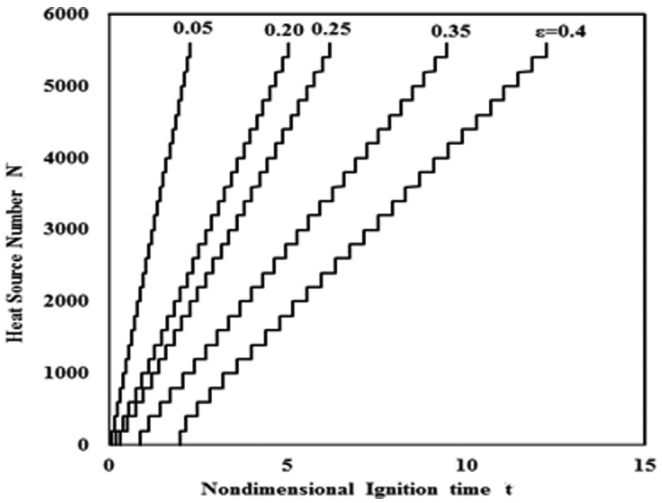

FIG. 3. Ignition time profiles of a discrete periodic system using Eq. (5) at different ignition temperatures.

the propagation of combustion front is strongly determined by the reaction kinetics.

The calculations and results shown till now were constrained to the discrete periodic system. Experimental studies have shown that the behavior of combustion process and burn rate changes with change in diluter and amount of diluter [1–6,12–15]. And the combustion front in actual system, when observed through high-speed microvideo, propagates roughly [5,12–15]. The role of randomness in internal structure of a discrete system is very well established from previous works [16–19,32–38]. Earlier theoretical models have considered the discrete disordered system and observed the kinetic roughening of combustion front [16–19]. However, the role of diorderness in structure of the discrete system was completely ignored. And the finger patterns in structure of combustion front were not observed. Hence, it is important to consider the role of randomness in the discrete adiabatic disordered system. And the role of diorderness in the propagation of combustion front is explained in the next section. However, the numerical experiments performed for the discrete periodic system using MPI programming are essential for validating code and to obtain the knowledge of optimized domain size for the disordered system. The optimized domain values (size of discrete system, periodic boundary) obtained from numerical experiments performed for periodic system is taken as operating conditions for the disordered system. Thus, the slice reconfiguration method can now be utilized for simulating the discrete disordered systems. The next section describes the realization of the disordered system, a method of varying the internal structure and numerical simulation of the disordered system.

C. Discrete disordered system

1. Realization of the disordered system

The internal structure of the discrete disordered system is shown in Fig. 5. The domain size of a two-dimensional discrete disordered system is 54×200 heat sources where $l_x = 54$ and $l_y = 200$ (similar to the discrete periodic system). Burnt point heat sources (represented by '●') are distributed periodically and unburnt cells (represented by '○') are arranged in random fashion. The value of periodic boundary (m) of the disordered system is same as that of the periodic boundary of periodic system.

The structure of actual powder system [1–8,12–15,32–42], which is formed during mixing and packing of heterogeneous mixtures, is *a priori* unknown, hence different realizations of the disordered systems are considered to understand the effect of disorderness on combustion behavior of the system. Such a detailed study for the effect of disorderness on mixing efficiency is completely neglected in the field of discrete combustion modeling. Different kinds of discrete disordered systems are built purposefully in the present work to address different behaviors of heterogenous mixtures that occur as a consequence of mixing and packing of actual mixtures. A variable frequency count method along X axis with the average inter-source spacing of unity is introduced for distributing unburnt heat sources. Each such distribution of unburnt heat sources in a two-dimensional plane correspond to a particular disordered system. About four discrete disordered systems each with an average sampling of around 40 sets are considered. The joint frequency count of 6000 unburnt heat sources of four such disordered systems is shown in Fig. 6. Figure 6(a) shows the joint frequency count of 30×200 unburnt heat sources. From Fig. 6(a) it can be observed that the unburnt heat sources are distributed nonuniformly along x axis and uniformly along y axis. The unburnt point heat sources are concentrated more in the middle region of the system. Physically, this situation can be seen when the mixture is densely packed in middle region of the combustion

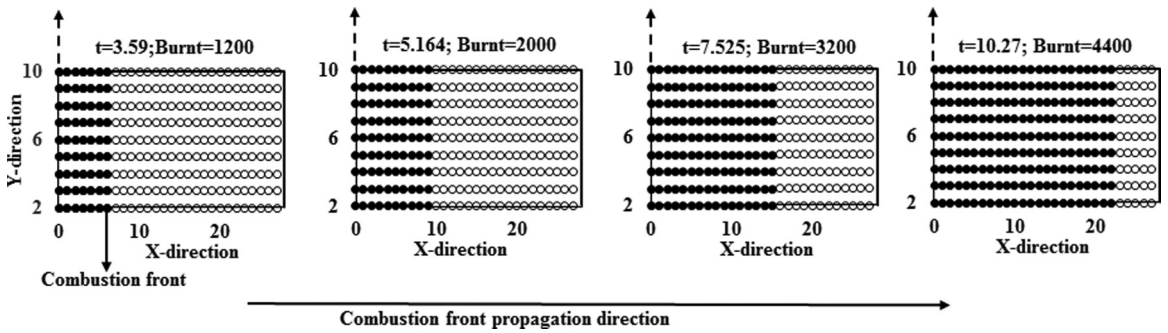

FIG. 4. Structure of combustion front in a discrete periodic system for ignition temperature (ε) = 0.4.

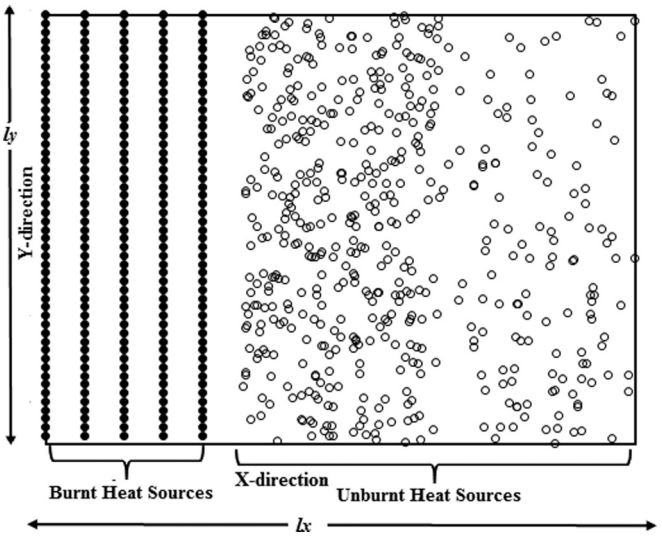

FIG. 5. Structure of the two-dimensional discrete disordered system. '●' represents the burnt particles and '○' is for unburnt particles.

chamber. Similarly, different possibilities that resemble actual packing are considered in the present model for modeling the internal structure of the discrete disordered system. The internal structure of the disordered systems is shown by joint frequency count shown in Figs. 6(b), 6(c), and 6(d). Figure 6(b) represents the joint frequency count for the disordered system S2. It can be observed that unburnt heat sources are densely packed in the initial region of the combustion chamber. This resembles to situation that is densely packed only in one end.

Figure 6(c) show the joint frequency count for disordered system S3. Here the unburnt heat sources are densely packed at the tail end of the system. Figure 6(d) represent the joint frequency count for disordered system S4, where the unburnt heat sources are densely packed at both ends of the unburnt heat sources of the system and loosely packed in the middle region of the system. This method of arranging unburnt heat sources in a two-dimensional disordered system is unique, interesting and useful in understanding the effect of change in internal structure on the combustion behavior. These four disordered systems S1, S2, S3, and S4 are now considered for the simulation of combustion process using Eq. (5).

2. *Results of the disordered system*

Disordered systems with different internal structures is simulated numerically by using the method MPI+slice reconfiguration. The numerical results obtained for the disordered system are explained here. Figure 7 shows the ignition time profiles of a disordered system S1, S2, S3, and S4 at different ignition temperatures. Figure 7(a) shows the ignition time profile for the discrete disordered system S1 at different ignition temperatures (ε). In the case of periodic system heat energy released travels in unique direction and hence unburnt heat sources in periodic system burn layer by layer as shown in Fig. 3. Whereas in the case of the discrete disordered system the heat energy released from burnt heat sources has to overcome the randomness in internal structure. Hence the unburnt heat sources are burnt randomly as shown

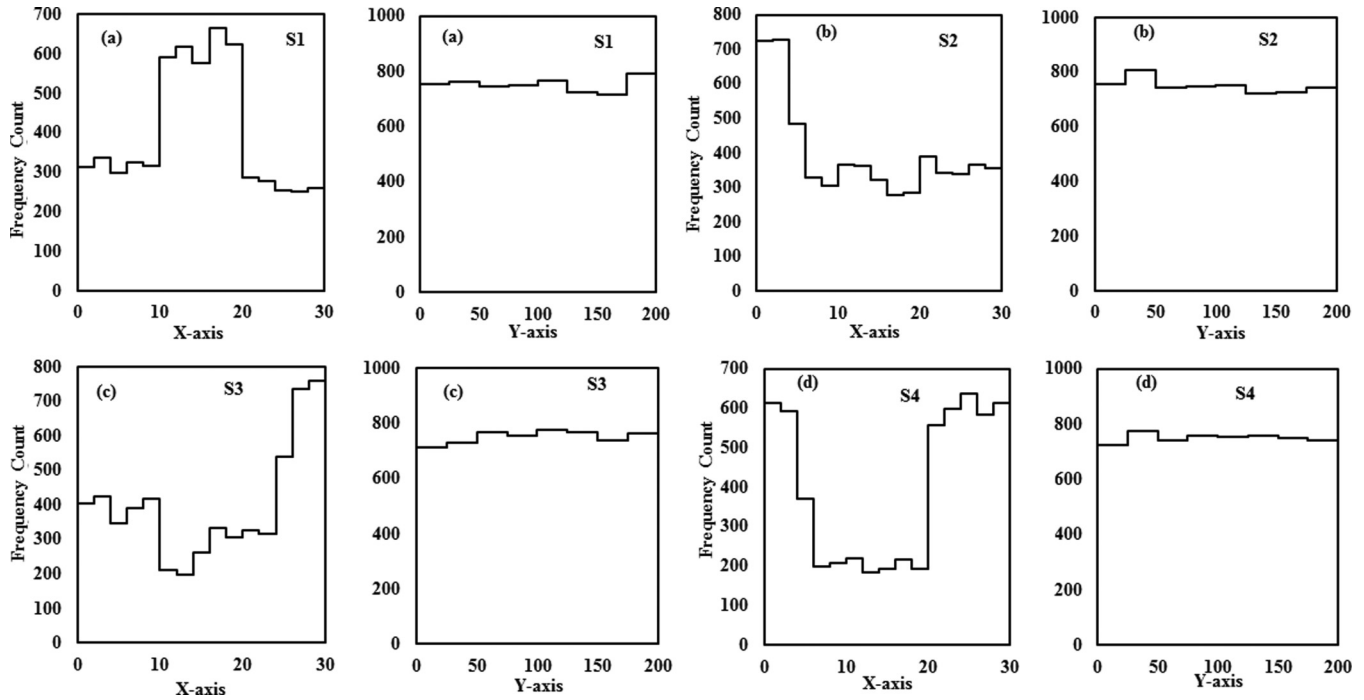

FIG. 6. Joint frequency count of 30 × 200 unburnt heat sources for different disordered systems. (a), (b), (c), and (d) in the figure represents distribution of x and y coordinates for different systems S1, S2, S3, and S4, respectively. S1 resembles those actual mixtures where the chemical components are more densely packed in the middle region of combustion chamber. Similarly, S2—densly packed in the initial part, S3—densely packed at the tail end, and S4—densely packed at initial and tail end of the combustion chamber.

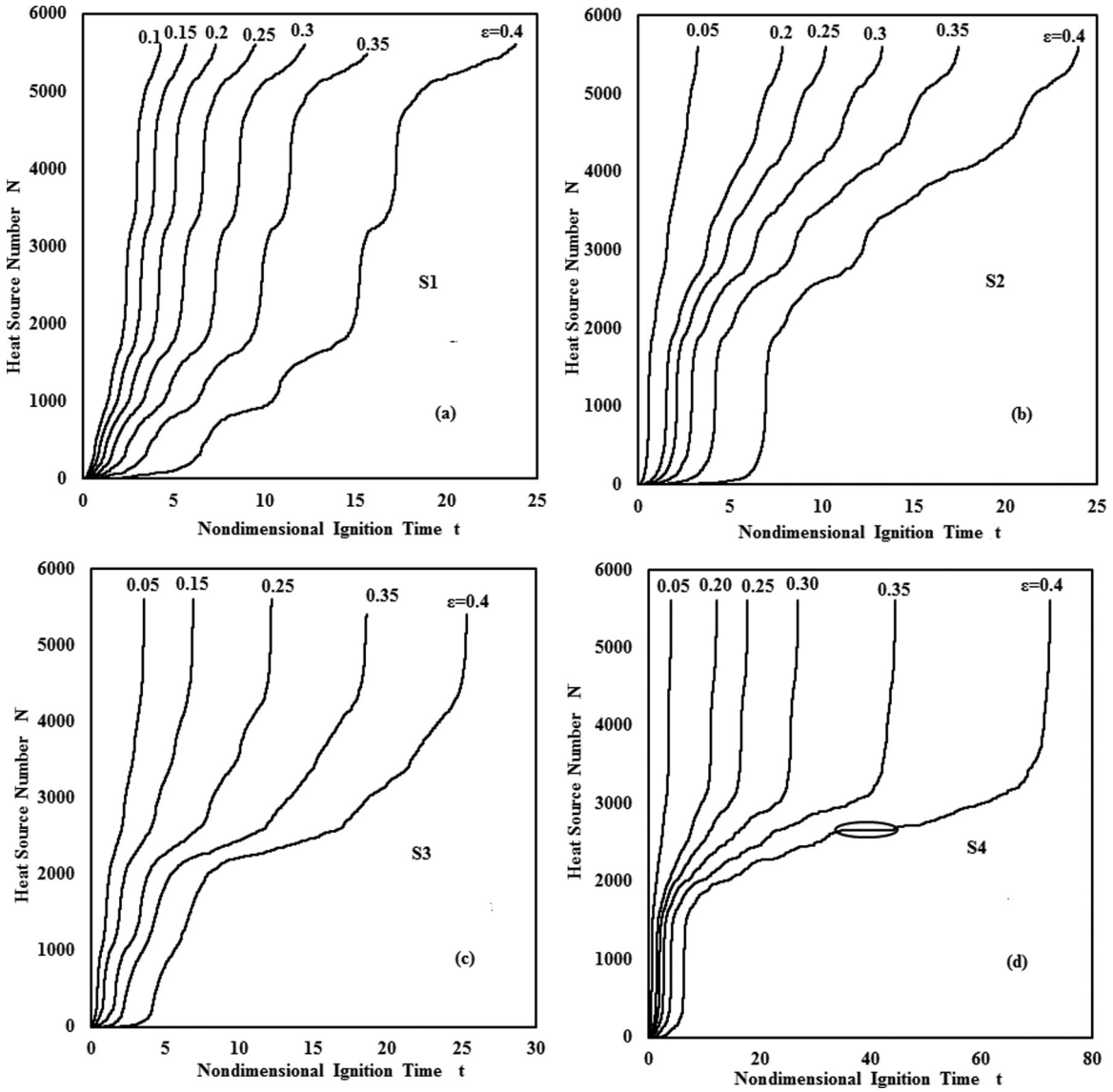

FIG. 7. Ignition time profile for discrete disordered systems S1, S2, S3, and S4 at different nondimensional ignition temperatures (ε). Circle represents the combustion stop.

in Fig. 7(a). At lower ignition temperatures ($\varepsilon < 0.15$) the available heat energy form burnt heat sources is self-sufficient and burning of unburnt heat sources occurs linearly. However, as ignition temperature increases ($\varepsilon > 0.15$) the random structure of the disordered system plays a crucial role and the burning of unburnt heat sources occurs in form of jumps. Similarly, the ignition time profiles for disordered systems S2, S3, and S4 are shown in Figs. 7(b)–7(d), respectively. It is interesting to observe from Figs. 7(a)–7(d) that the ignition time (t) for burning the unburnt heat sources increases with increase in ignition temperature and randomness in internal structure of the system. Ignition time profile for the disordered system is linear at lower ignition temperatures for all systems S1, S2, S3, and S4. The circle in Fig. 7(d) for a disordered system S4 represent the occurrence of combustion stop at ignition temperature (ε) = 0.4. At higher ignition temperatures (ε) = 0.4 burning occurs in form of consequent jumps: relatively long periods of front stopping (induction periods) are followed by the burning-out of some part of the sample with practically constant burning rate and followed by a new induction period again. Duration of induction periods and periods of "continuous" combustion are random and it is connected with the random structure of the system [16–19,32–38]. As the reaction front propagate and reach final stage of burning the accumulation of heat energy decreases and thus leads to self-slow heating of the mixture. Similarly, the experimental data on combustion of powder mixtures [1–6,14] show that the process of reaction front propagation in actual systems is random [16–19,32–38] and is accompanied by fluctuations in flame structure and burning rate of system as a whole. The fluctuations observed in ignition time profiles are result of both random microstructure and nonlinearity of the system.

In experiments [5,14], the change of mixture and concentrations parameters of powder components (e.g., a changing in stoichiometric coefficient x in mixture Ti + xSi) results in either regularization or stochastization of combustion process. A similar behavior of burning front is observed from the

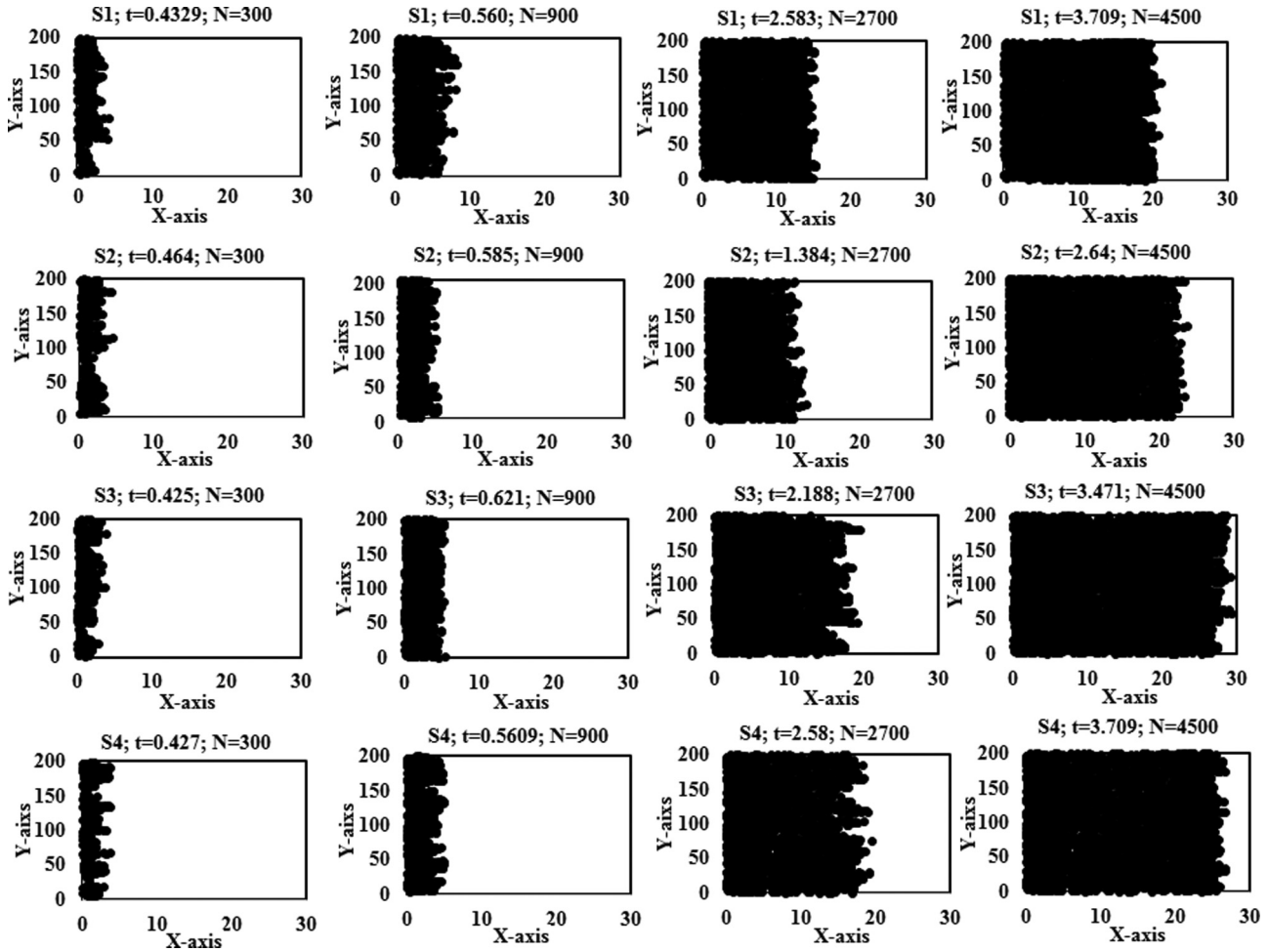

FIG. 8. Snapshot of instantaneous combustion front for ignition temperature $\varepsilon = 0.05$ with burnt heat sources 300, 900, 2700, 4500 at different ignition times for different disordered systems S1 (first row), S2 (second row), S3 (third row), and S4 (fourth row). S1—structure of combustion front shifts from irregular to regular pattern. S2—regular to irregular. S3—sparse fingers. S4—chaotic fingers.

present model. In numerical experiments the regularization (at lower ignition temperatures) results in less fluctuations of duration of induction periods and process becomes more stable, and the stochastization (at higher ignition temperatures) results in when combustion becomes more random one with long and random induction periods. The process is more regular at smaller ε and less randomness in structure; more ε and more randomness the more random is the combustion process, the stronger effect of fluctuation of random structure of system on the burning front propagation. The results in Fig. 7 show the method of packing the powder mixture, that automatically forms the internal structure of the discrete disordered system, results in change in reaction kinetics, and effects the combustion process.

In the case of the discrete periodic system, the combustion front propagates in layer by layer (planar pattern) as shown in Fig. 4. This is because of the availability of self-sustained heat energy throughout the system. It is important to note that the combustion front or burn front for actual systems [9–11,25–31] when observed through HSMV is observed to be propagating in an irregular pattern. The irregularities in the pattern of combustion front are driven by the uncertainty of the reaction zone. Different patterns of combustion front, such as stable, irregular, periodic, fingering pattern with tip splitting, and fingering pattern without tip splitting, are observed during experiments [9–11,25–31]. Similar patterns of the combustion front can be observed from the present two-dimensional discrete disordered system as shown in Figs. 8, 9, 17, and 18. Figure 8 shows the snapshots of combustion front for an ignition temperature $(\varepsilon) = 0.05$ at different ignition times for different disordered systems S1, S2, S3, and S4. Figure 8 shows the structure of combustion front at different ignition times for four samples S1, S2, S3, and S4 at ignition temperature $\varepsilon = 0.05$. The snapshot of instantaneous combustion front is captured after following number of unburnt heat sources $N = 300$, 900, 2700, and 4500 are burnt. The first row in Fig. 8 shows the structure of combustion front propagating in x direction from left to right for discrete disordered system S1 at different ignition times. Initially the structure of combustion front is irregular after 300 and 900 unburnt heat sources have burnt at ignition times 0.4329 and 0.56, respectively. However, it is interesting to observe that the structure of the combustion front becomes regular as the front reaches the middle region of the system. This is because of the unburnt heat sources that are densely packed in the middle of the system as shown in Fig. 8(a) for discrete disordered system

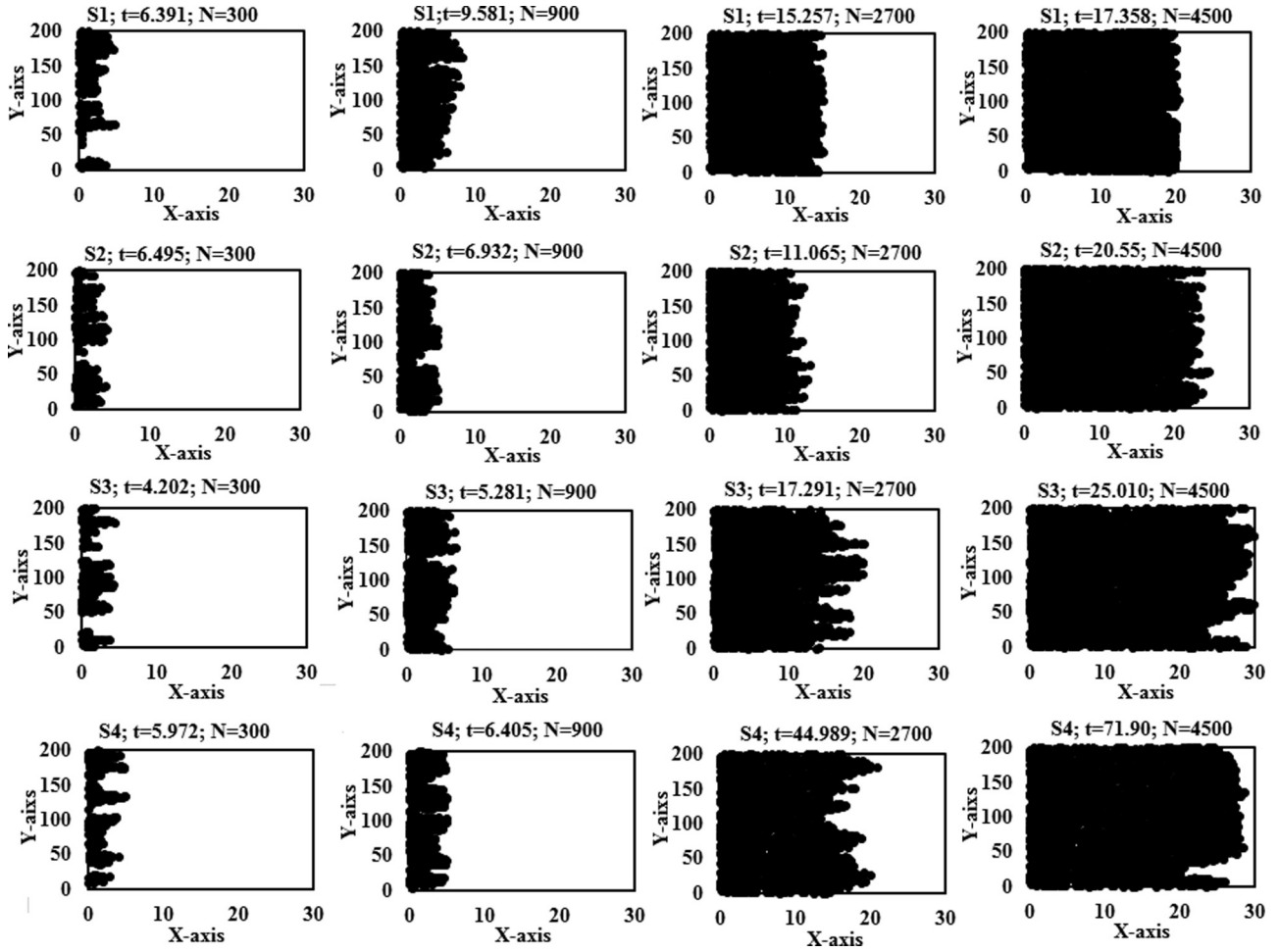

FIG. 9. Snapshot of instantaneous combustion front for ignition temperature $\varepsilon = 0.4$ with burnt heat sources 300, 900, 2700, 4500 at different ignition times for different disordered systems S1 (first row), S2 (second row), S3 (thirrd row), and S4 (fourth row). S1—irregular to regular combustion front. S2—irregular and increased fingers. S3—fingers with tip split. S4—increased chaotic fingers.

S1. The change of structure of combustion front from irregular to regular is related to sudden change of reaction kinetics. The second row in Fig. 8 represents the snapshot of combustion front for disordered system S2. The structure of combustion front is regular after burning 300 and 900 unburnt heat sources at ignition times 0.464 and 0.585, respectively. However, as a greater number of unburnt heat sources are burnt, the structure of combustion front becomes rough. The third row in Fig. 8 shows the snapshot of combustion front for disordered system S3. The structure of combustion front after burning 2700 unburnt heat sources becomes irregular characterized with fingering patterns. The fourth row in Fig. 8 represents the structure of combustion front for disordered system S4. The structure of combustion front is irregular with fingering patterns. Different disordered systems S1, S2, S3, and S4 at the same ignition temperature 0.05 show different combustion behavior with different combustion front structure, which indicates that the internal structure of the disordered system effects the combustion process.

Structure of combustion front for different disordered systems at the same ignition temperature$(\varepsilon) = 0.05$ is observed to be different, and propagation of combustion front is affected by change in internal structure of the system. Projections of combustion front fingers can be observed at different locations in the system. It can be detected from Fig. 8 that the irregularity in combustion front increases with an increase in uncertainty of the system structure even at lower ignition temperatures (ε). The trend of increase in disorderness in the discrete disordered system can now be represented by S1 $<$ S2 $<$ S3 $<$ S4. Here heterogeneity in the internal structure of the disordered system plays a crucial role by creating the uncertainty in the reaction zone and destabilizing the reaction front.

Different fingering-like patterns observed during experiments [9–11,25–31] are also reproduced using the present discrete disordered system. In experimental works [9–11,25–31], where different combinations of fuel and oxidizer are mixed together and ignited, the combustion front is recorded and analyzed. This process of obtaining the structure of combustion front is tedious, time consuming and costly. In the present developed model different possibilities of joint frequency count are utilized to obtain different discrete disordered systems. Combustion behavior of each such disordered system resembles to different actual systems (characterized by different diluter and different percentage of diluter).

Figure 9 represents the structure of combustion front for ignition temperature $(\varepsilon) = 0.4$ at different ignition times for discrete disordered systems S1, S2, S3, and S4. As the

ignition temperature increases the heat energy available from all unburnt heat sources decreases and the combustion front propagates with instabilities as observed from rows 1,2 3, and 4 of Fig. 9. It can be noted from Fig. 9, when compared to Figs. 8, 17, and 18, that the length, width, and spacing of fingers increases with increase in randomness of the system. S1 is the less disordered and S4 is a highly disordered system. Increase in spacing and length of the fingers are more detected at higher ignition temperatures.

In the previous experimental works [9–11,25–31] it was reported that the fingering pattern is related to reactant transport and the width of the finger is determined by heat loss. However, it is very interesting to observe from Figs. 8, 9, 17, and 18 of present discrete model that the randomness in structure of discrete system plays a crucial role in deciding the structure of combustion front even in the absence of heat loss. The internal structure which is automatically formed during the packing of heterogeneous mixture is addressed in present model using the method of joint frequency count. And different possibilities of joint frequency count are utilized for obtaining different discrete disordered systems. Hence, the role of randomness in discrete disordered systems plays a crucial role in the behavior of combustion.

3. Width of the combustion front

The present section describes about the effect of disordered structure on the mean width (w) of the instantaneous combustion front for different discrete systems S1, S2, S3, and S4 at different $\varepsilon = 0.05$, 0.20, 0.30, and 0.40. The mean width (w) of instantaneous combustion front of the discrete system shown in Fig. 10 is measured by searching the location of burnt heat source $w_i(x,t)$ of all projections of combustion front at different ignition times.

The mean width of combustion front grows indefinitely with time. However, as the randomness and ignition temperature increase progressively the mean width of the combustion front grows randomly with notable initiation and domain size effect. The mean width of the combustion front at $0.05 < \varepsilon < 0.40$ follows the trend S1 > S2 > S3 > S4. The dashed circle in Fig. 10 represents the initiation effect and circle represents the domain size effect. The initiation effect in the discrete system, because of the heat energy available from the burnt heat sources, ensures for the self-sustained propagation of combustion front. Surprisingly, the duration of initiation effect decreases with increase in ignition temperature and domain size effect is predominantly observed for discrete system S4 at $\varepsilon > 0.05$.

4. Roughness of the combustion front

The present section describes about the effect of disordered structure on the roughness (R) of the instantaneous combustion front for different discrete systems S1, S2, S3, and S4 at different $\varepsilon = 0.05$, 0.20, 0.30, and 0.40. The roughness of the combustion front is given by the maximum deviation of finger projection from the mean width of combustion front (w). The roughness of combustion front (R) for discrete system S1, S2, S3, and S4 is shown in Fig. 11 with different symbols. The roughness of the combustion front increase with increase in randomness and ε.

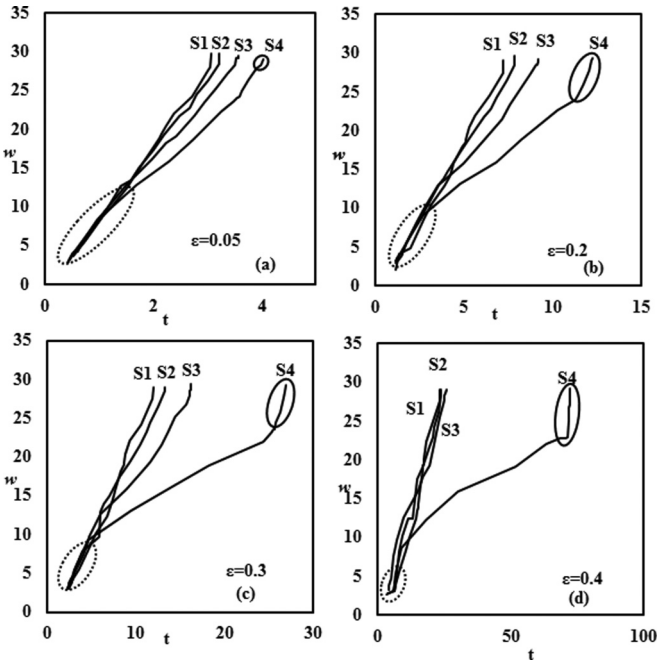

FIG. 10. Width of the instantaneous combustion front for discrete system S1, S2, S3, and S4 at different ignition times and different ε: (a) $\varepsilon = 0.05$, (b) $\varepsilon = 0.20$, (c) $\varepsilon = 0.30$, (d) $\varepsilon = 0.40$. Dashed circles represent the initiation effect and circles represent the domain size effect.

The roughness of combustion front observed for discrete system follow the trend S1 > S2 > S3 > S4. The deviation of the roughness indicates the increased intensity of fingering patterns. The intensity of fingering pattern is more pronounced for S4 and higher values of ε. It is very interesting to observe that the roughness (R) for all discrete system is more pronounced in the middle region of the combustion chamber which indicates the higher uncertainty of the reactions. Whereas at the initial and tail region of the combustion chamber the roughness decreases because of the presence of initiation and domain size effect.

D. Burn rates

Burn rate is an important physical parameter that quantifies the rate of propagation of combustion front. Hence it is crucial to understand the burn rate at different ignition temperatures and for different discrete system. Burn rates at different ignition temperatures are calculated using Eqs. (5) and (6) for discrete periodic and different discrete disordered systems. The comparison of burn rates for periodic and disordered systems S1, S2, S3, and S4 (each 40 sets) are shown in Fig. 12. Each single point shown in Fig. 12 is obtained by using slice reconfiguration scheme, which otherwise would be difficult and time consuming to calculate by considering total unburnt particles. Burn rates are plotted with standard deviation for each discrete disordered system. Reaction kinetics are very quick and spontaneous at lower ignition temperature. Hence, burn rate at lower ignition temperatures are very high when compared to burn rates at higher ignition temperature. This spontaneous reaction kinetics also cause fluctuations in

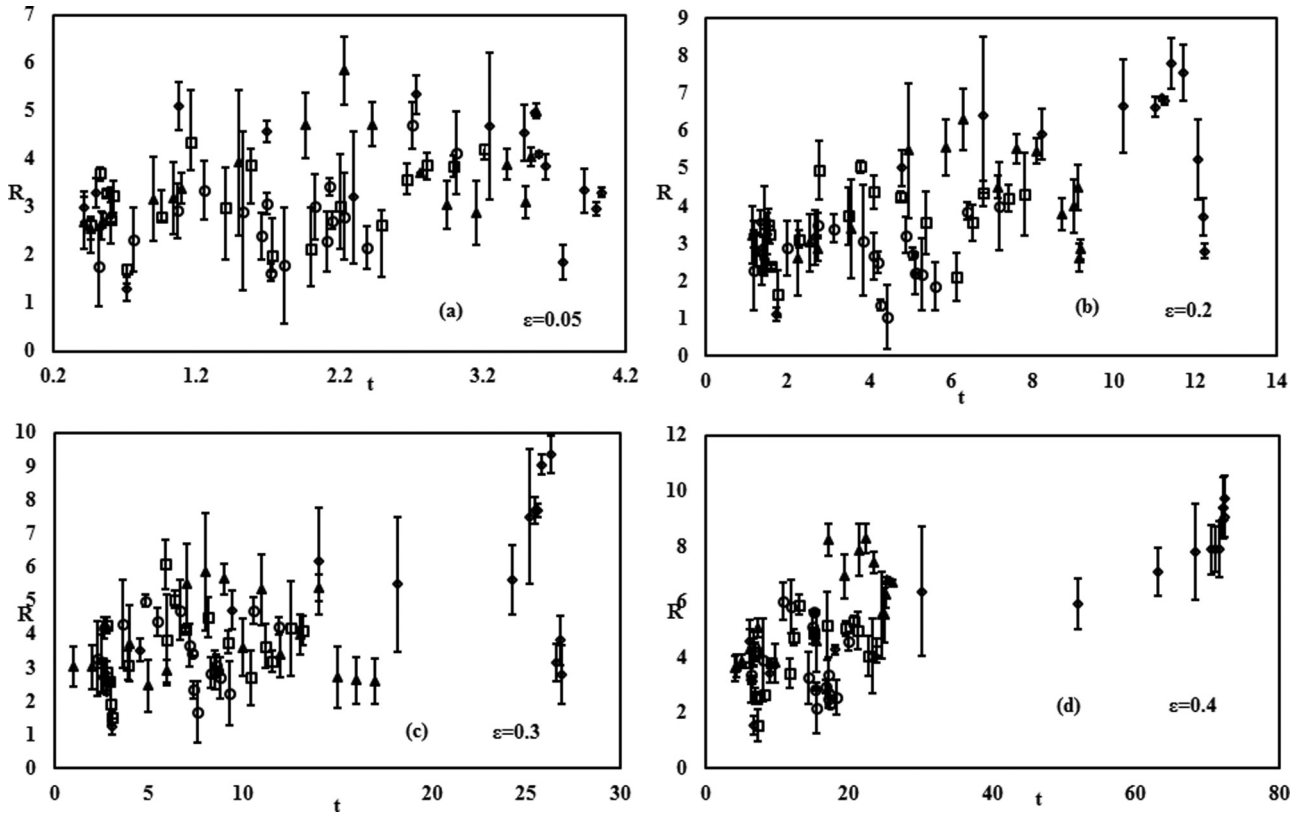

FIG. 11. Roughness of the combustion front for discrete systems S1, S2, S3, and S4. (a) $\varepsilon = 0.05$; (b) $\varepsilon = 0.20$; (c) $\varepsilon = 0.30$; (d) $\varepsilon = 0.40$. Symbols '○' represent S1, '□' represent S2,'△' represent S3, and '◇' represent S4. Deviation indicates the intensity of fingering patterns.

burning of heat sources for each discrete disordered system. Hence, it can be noted from Fig. 12 that standard deviation of burn rate is high at lower ignition temperatures and decreases with increase in ignition temperature for each disordered system. Experimental data [5,14] show that the burn rate is affected with change in burning temperature. Similarly, Fig. 12 shows that the burn rates decrease with increase in ignition temperature for a discrete system. Experimental data [5,14] also report that the burn rate changes with change in diluter and percentage of diluter.

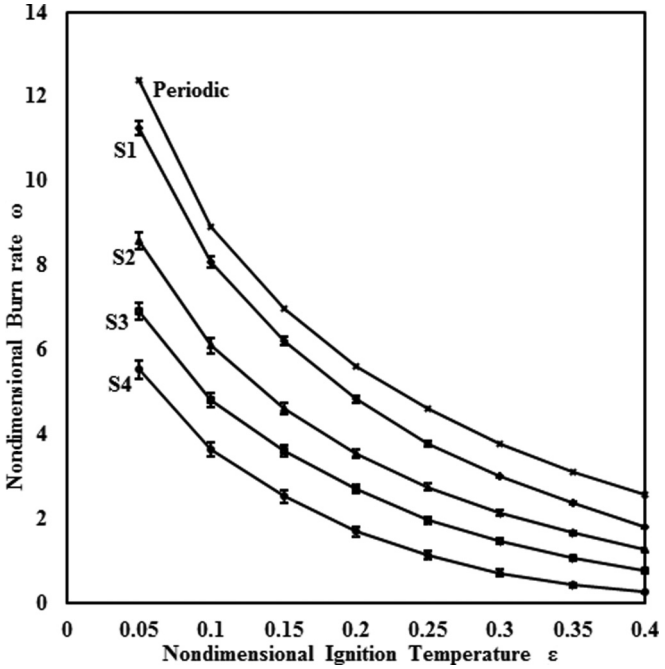

FIG. 12. Comparison plots of burn rates calculated for periodic and disordered systems using Eqs. (5) and (6).

Similarly, from the present model as shown in Fig. 12 it can be observed that at each ignition temperature as the randomness in discrete system increases the burn rate decreases. It is interesting and important to observe that the burn rates of a disordered system are less than the periodic system. The random internal microstructure of the discrete system can play a crucial role in the combustion process and should be taken into account in the modeling of combustion of heterogeneous systems. Thus, knowing that burn rate changes with change in internal structure and ignition temperature of the system can help the combustion designer in successful design of the heterogeneous mixture.

E. Comparison with experimental data

Figure 13 shows the comparison plot for burn rate and burning temperature for different powder mixture performed by Doryvankin *et al.* [5]. Different symbols in Fig. 13 represent the burn rates of different powder mixture. It can be observed from Fig. 13 that the burn rate for each powder mixture decreases with increase in burning temperature. And

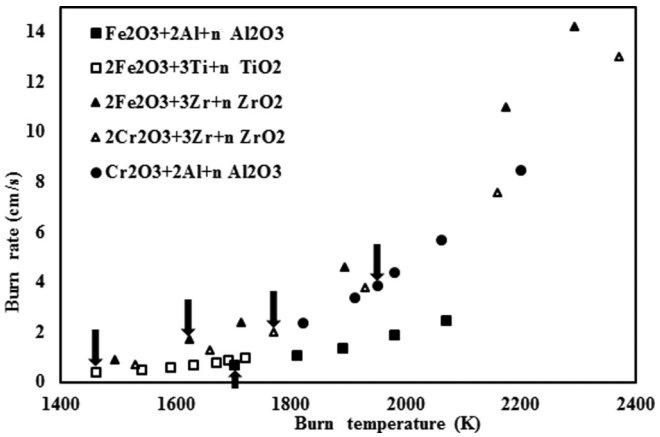

FIG. 13. Comparison plots of burn rates for different thermite mixture obtained from previous experimental work [5].

the arrow marks represent the commencement of unstable combustion. The experimental work on powder mixture shows that the burn rate of a mixture varies with change in diluter and also with change in percentage of the diluter (n). These observations from the previous works show that the combustion process and its behavior is affected with change in diluter.

Prediction of burn rate of powder mixtures with change in burning temperature and change in diluter is unexplored till now. In this section, the behavior of such mixtures is explained in the view of present discrete model. The treatment of experimental data as shown in Fig. 13 with the dimensional coordinates burn rate (r) and burning temperature (T) are now processed in the nondimensional co-ordinates burn rate (ω) and ignition temperature (ε). The work reports the critical

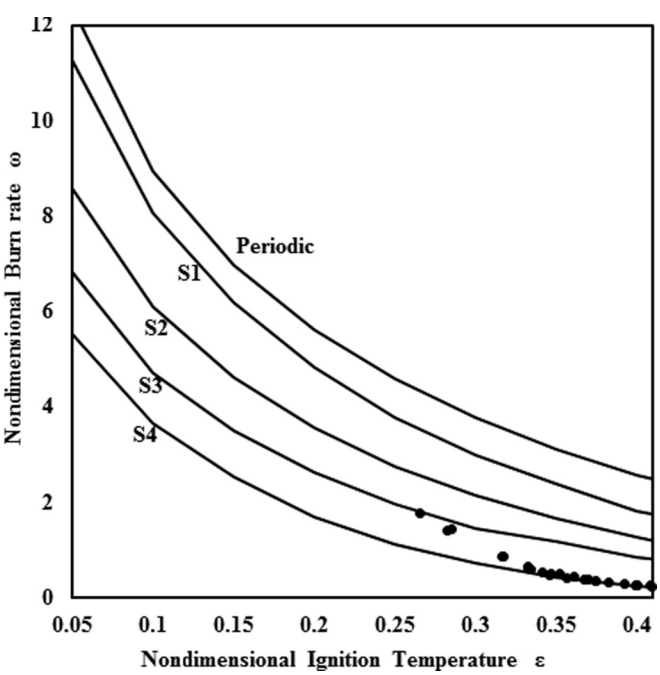

FIG. 14. Comparison plots of burn rates calculated from present model (represented by solid line) and experimental work [5] (represented by symbol).

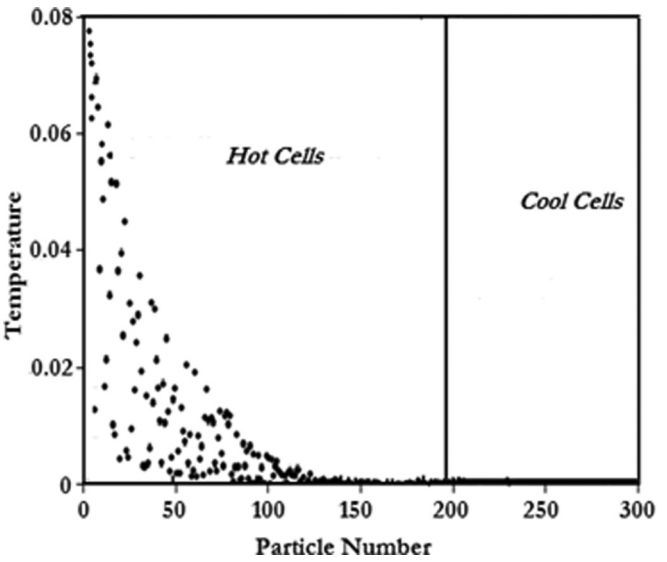

FIG. 15. Temperature profile for unburnt cells.

values, of burn rate (r_{cr}) and burning temperature ($T_{ad_{cr}}$), at the commencement of unstable combustion. Similarly, these critical values are obtained from present model at the onset of unstable combustion. The onset of unstable combustion in the present model is noticed with oscillations and stops in combustion wave. The percentage of diluter and change of diluter practical in experiments is now correlated with joint frequency count of the discrete disordered system of the present model. Assuming the critical values of rate of burning (r_{cr}) and burning temperature ($T_{ad_{cr}}$), measured in experiments, correspond to commencement of oscillating modes of combustion process

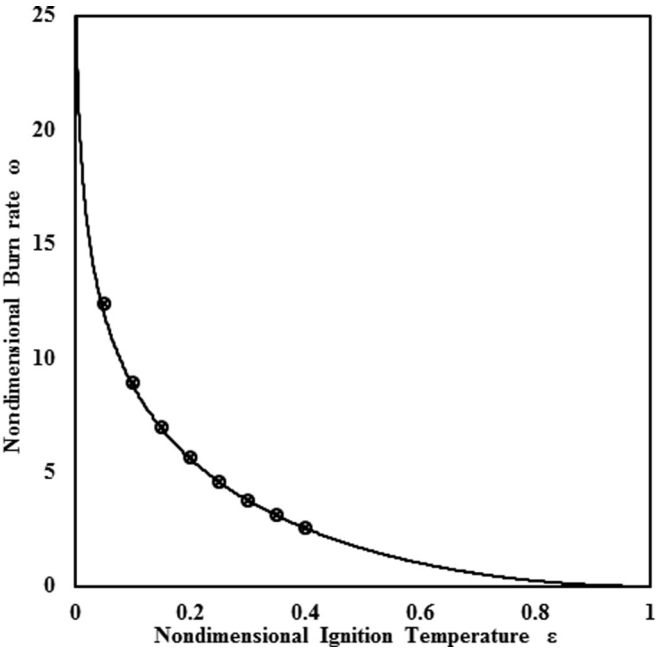

FIG. 16. Comparison plot for burn rates of a discrete periodic system. Solid line is obtained using Eq. (7) and symbols are obtained using Eqs. (5) and (6). "o" represents numerical burn rates using MPI and "x" using MPI and slice reconfiguration scheme.

TABLE I. Comparison of computational time of the discrete periodic system using Eq. (5) by both methods for ignition temperatures $(\varepsilon) = 0.05$–0.4.

		Computational time (min) using Methods	
Ignition temperature (ε)	Number of Cores	Total combustible system with MPI (min)	Slice reconfiguration with MPI (min)
0.05	2×20	35	1.1
0.10	2×20	42	1.32
0.15	2×20	48	1.44
0.20	2×20	52	2.11
0.25	2×20	61	2.56
0.30	2×20	70	3.33
0.35	2×20	90	4
0.40	2×20	118	5

for an actual system. Using the recommendation of the present theory,

$$\varepsilon = \varepsilon_{\rm cr} \frac{T_{\rm ad_{cr}} - T_{\rm in}}{T_{\rm ad} - T_{\rm in}}, \tag{8}$$

$$\frac{\omega}{\omega_{\rm cr}} = \left(\frac{r}{r_{\rm cr}}\right)\left(\frac{l_o}{l_{o_{\rm cr}}}\right), \tag{9}$$

$$\left(\frac{l_o}{l_{o_{\rm cr}}}\right)^3 = \frac{1 - n_{\rm cr}}{1 - n}. \tag{10}$$

The dimensional coordinates of burn rate and burning temperature of the previous experimental data is now converted in to nondimensional coordinates ε-ω as shown in Fig. 14 (represented by symbol '●'). Similar observations of the actual combustion process and burn rate can be reproduced from the present model. Only on the assumption that the internal structure of the discrete system is related with change in diluter and also with change in percentage of diluter. Solid lines in Fig. 14 represent the burn rate obtained for discrete periodic and disordered systems S1, S2, S3, and S4.

It can be noted from Fig. 14 that the discrete disordered system S4 completely agrees with the experimental work at higher ignition temperatures ($\varepsilon > 0.3$). Whereas the discrete system S3 agrees with experimental work [5] at lower ignition temperature ($\varepsilon < 0.3$). This indicates that the reaction kinetics at lower ignition temperature are very spontaneous and, in such situations, the discrete system S3, with less disorderness in internal structure when compared to that of S4, can explain the actual combustion process. In addition, it is important to observe that at higher ignition temperatures the behavior of combustion process is very uncertain and can be predicted by the most disordered discrete system S4.

The two-dimensional discrete adiabatic combustion model with the incorporation of joint frequency method is very efficient and flexible in describing the actual propagation of combustion front. The computer based indigenous modeling using MPI programming facilitated faster computation and detailed diagnosis of two-dimensional combustion wave. The multifold improvement in computation time with accuracy of such discrete system is obtained by the method of slice reconfiguration scheme using MPI programming. Earlier works [9–11,25–31] have shown that the heat loss causes instabilities in the propagation of combustion front with the manifestation of fingering patterns. The results from present model interestingly indicates that this is not always the case because even in the absence of heat loss the disorderness in internal structure of the discrete system play a crucial role and cause instabilities in the propagation of combustion front with the manifestation of irregular patterns. The proposed model also shows that the internal structure, which is formed automatically during mixing the actual heterogeneous mixture, leads to the irregular propagation of combustion front with voids, sparse fingers, splits in fingertip, and chaotic fingers. The internal structure of a discrete system causes the fluctuation in reaction kinetics, which in turn effects the combustion process. This result from the proposed model is very interesting because the utilization of joint frequency count method in describing the internal structure of the discrete system leads to the different destabilized combustion fronts. The advantage with discrete two-dimensional modeling is that it visualizes the structure of combustion front for all ranges of mixing from periodic to highly disordered. While the results in the present work were concentrated only in the range of $\varepsilon < 0.4$, nevertheless, the present model could report interesting results of combustion phenomenon. These results from the present work can serve the purpose of preliminary understanding the effect of internal structure on combustion process. The present method of study will be extended to three-dimensional modeling of combustion and ignition temperatures ($\varepsilon > 0.4$) in future. In this direction the study can report the behavior of the combustion process in the unstable and also the combustion limit.

IV. CONCLUSION

In this work, the effect of disorderness in two-dimensional discrete adiabatic combustion wave is investigated in detail by modeling and performing the numerical experiments for two systems, namely, (i) periodic and (ii) disordered. In the case of the discrete periodic system, staircase ignition time profiles are observed. The propagation of combustion front is determined strongly by the reaction kinetics as a consequence of linear interaction of the structure of the periodic system and the combustion wave. Such an interaction creates the layer-by-layer feature of combustion wave propagation for nondimensional ignition temperatures ($\varepsilon < 0.4$).

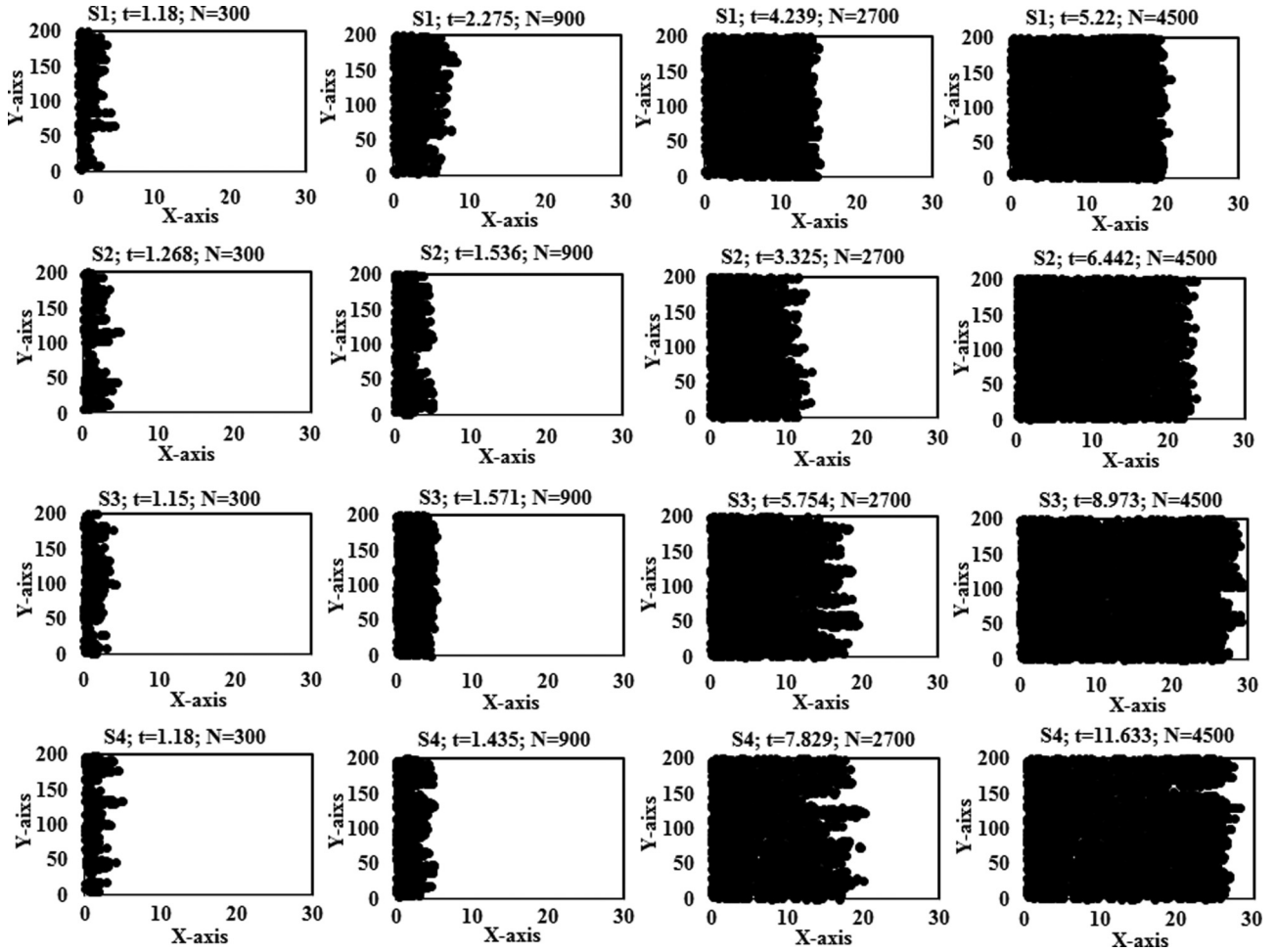

FIG. 17. Snapshot of instantaneous combustion front for ignition temperature $\varepsilon = 0.2$ with burnt heat sources 300, 900, 2700, 4500 at different ignition times for different disordered systems S1 (first row), S2 (second row), S3 (third row), and S4 (fourth row). S1—irregular fingers to regular combustion front. S2—sparse fingers. S3—sparse fingers with increased roughness. S4—chaotic fingers with increased roughness.

The incorporation of the joint frequency count method facilitates the proposed model to work from uniform (S1) to most random (S4) discrete disordered systems. In the case of the discrete disordered system, the ignition time fluctuates with pronounced ignition delays. Propagation of combustion front is strongly affected by the rate of heat transfer among the cells as a result of nonlinear interaction of the internal structure of heterogeneous mixture and the combustion wave. This interaction creates the instabilities and irregular features in the structure of instantaneous combustion front even for constant ignition temperature. When the randomness in structure of the discrete system increases, the combustion front propagates irregularly with sparse and chaotic fingers. Irregular, periodic, sparse fingers, and chaotic fingers in combustion front patterns as observed during experiments are reproduced with the proposed discrete disordered model only. The voids in structure of combustion front observed in experiments is corroborated by the present two-dimensional disordered system only for $\varepsilon > 0.3$. The width of the fingers and spacing between fingers increase with both ignition temperature and randomness in discrete system. The average width of combustion front increases indefinitely with time. Initiation effect decrease with increase in randomness and ε manifesting unstable combustion fronts. Roughness and intensity of fingers of combustion front increase with randomness and ε.

It is found that the average burn rate of the disordered system is always less than the periodic system and follows the trend: periodic $>$ S1 $>$ S2 $>$ S3 $>$ S4 for $\varepsilon < 0.4$. The discrete disordered system S4 agrees well with experimental data for $\varepsilon > 0.3$, and system S3 agrees with experimental data for ignition temperatures $\varepsilon < 0.3$. The present study indicates decisively that the disorderness in the structure of heterogeneous mixture is very critical for modeling and predicting burn rate, which is essential for better understanding of the intricate process involved during the propagation of combustion front.

ACKNOWLEDGMENTS

The authors kindly acknowledge the funding from the Department of Aerospace Engineering and also the computational facility at the Computer Center, IIT Kanpur.

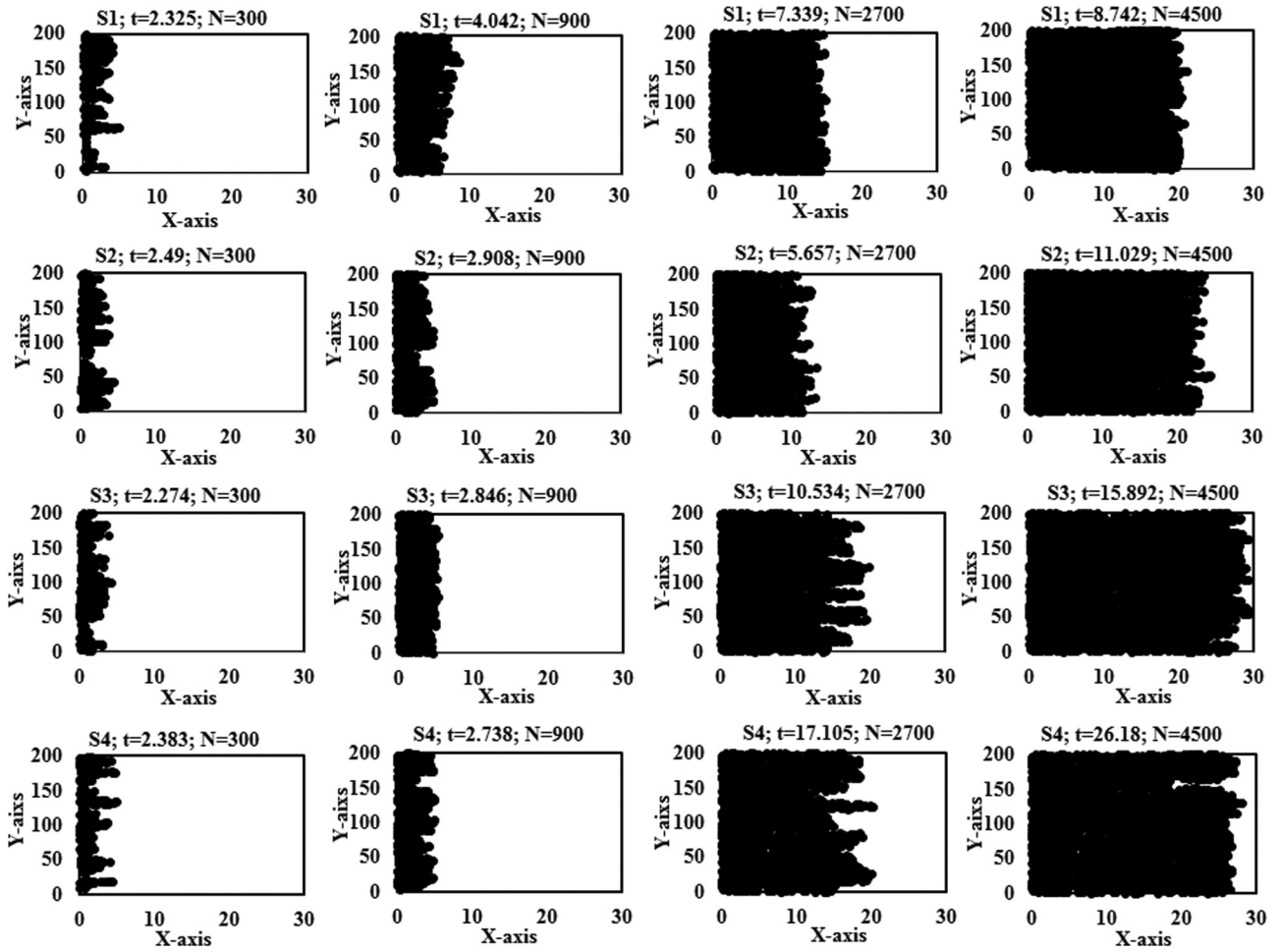

FIG. 18. Snapshot of instantaneous combustion front for ignition temperature $\varepsilon = 0.3$ with burnt heat sources 300, 900, 2700, 4500 at different ignition times for different disordered systems S1 (first row), S2 (second row), S3 (thirrd row), and S4 (fourth row). S1—irregular to regular combustion front. S2—irregular with increased number of fingers. S3—increased fingers and roughness. S4—increased roughness and chaotic fingers.

APPENDIX: FASTER COMPUTATION BY USING MPI

The MPI programming is utilized by distributing the work to different cores and collecting the data in synchronization. The MPI programming is executed in an HPC machine using 40 cores. The computation load on each core increases with increase in burnt and unburnt cells and parameter of periodic boundary along the y axis for each ignition time. Since the effect of burnt cells on unburnt cells cannot be ignored, the burnt cells cannot be shared or parallelized among cores. Hence, the unburnt cells are task parallelized. Here the total unburnt cells that undergo numerous loop iterations are distributed among the slave cores by master core. Slave cores are assigned with the computation of temperature of shared unburnt cells in synchronization. Master core gathers the temperature value of unburnt cells calculated by each slave core and compares the same with predetermined ignition temperature (ε). Simulation of combustion process using MPI programming cuts down the computation time to a great extent when compared to the computation time of the C program. However, for each nested iteration of periodic boundary (m), time increment and burnt cells the size of total unburnt reaction cells is of computational concern, and it is of interest to further reduce the computational time. Hence, the slice reconfiguration scheme is proposed.

A. Slice reconfiguration scheme

The slice reconfiguration scheme is proposed based on monitoring the temperature profile of unburnt point sources. The vicinity of reaction front distinguishes total unburnt cells in to two regions of reaction zone (Hot cells) and cool cells as shown in Fig. 15. Hot cells (reaction zone) are highly sensible to ignite and release heat instantly even for little increase in heat energy. The percentage of hot cells with effect to burnt cells is around 20–25% of the total unburnt cells. The cool cells comprise unburnt cells with low temperature and can be ignored until a single hot cell is burnt. Consequently, the total unburnt region is now reduced to

hot cells (slice) at each nested iteration for j and ignition time.

The slice is reconfigured time and again only after the temperature of the cell has attained the predetermined ignition temperature (ε). The above step is repeated until all unburnt cells are burnt. Considering the hot cells, the computation load on each core is now reduced as the sizes of unburnt cells are reduced to hot cells. The comparison for the burn rates of the discrete periodic system computed by MPI program and slice reconfiguration schemes using Eqs. (5) and (6) is shown in Fig. 16. The burn rates calculated from theoretical Eq. (7) for periodic system shown in Fig. 1 (represented by solid line) is taken as reference for validation of numerical burn rates [calculated by Eqs. (5) and (6)] obtained by two methods: one is considering a total (MPI program represented by symbol "**o**") combustible system and the second proposed method (slice reconfiguration represented by symbol "**x**"). Figure 16 shows that the numerical burn rates of a discrete periodic system calculated using MPI program and slice reconfiguration scheme completely agrees with the theoretical burn rates.

As ε increases, the burn rate decreases. This observation is similar to that of experimental results reported for the role of amount of inert diluter on burning time of thermite mixtures [5,12–15]. In the view of slice reconfiguration scheme the computational time is improved to multifold ($<$15 times). Considering the temperature profile of unburnt cells as shown in Fig. 15, the total number of unburnt cells is now reduced to hot cells (around 20% of total unburnt cells) for the calculation of temperature at each time. This step is performed until all the unburnt cells are burnt. The comparison of computational time for the discrete periodic system of the domain 54×200 heat sources (burnt and unburnt) by two methods is shown in the Table I.

B. Combustion front

Similarly, Fig. 17 shows the structure of combustion front obtained at ignition temperature (ε) = 0.2 for the discrete disordered systems S1, S2, S3, and S4.

As the ignition temperature increases an interesting feature in structure of combustion front can be observed as shown in Fig. 17. The randomness in internal microstructure for disordered system S1 have less effect on combustion front structure when compared to that of the disordered systems S2, S3, and S4. It can be noted from rows 2, 3, and 4 in Fig. 17 that the irregularities in combustion front now take the shape of fingers. Irregular fingering pattern and increase in the width of the fingers are observed for disordered systems S2, S3, and S4. The length of the fingers and number of fingers in combustion front increases with increase in random structure of the system. In actual systems the finger width is determined by the ability of reaction front to release heat [9–11,25–31]. Similarly, in the proposed model it can be inferred that increase in the ignition temperature and randomness in structure of the disordered system causes decrease in the heat release from burnt heat sources and hence the destabilized reaction front starts exhibiting the fingering patterns even at lower ignition temperatures. Figure 18 shows the structure of combustion front captured at ignition temperature (ε) = 0.3 at different ignition times for the discrete disordered systems S1, S2, S3, and S4. It can be observed from rows 1, 2, 3, and 4 of Fig. 18 that the irregularities in structure of the combustion front increase with increase in randomness of the system. It can be noted from Fig. 18, when compared to Fig. 17, the length, width, and spacing of fingers are increased. This indicates that the randomness in internal structure of the discrete disordered system plays a crucial role at higher ignition temperatures.

[1] A. S. Mukasyan and A. S. Rogachev, Prog. Energy Combust. Sci. **34**377 (2008).

[2] A. Varma, A. S. Rogachev, A. S. Mukasyan, and S. Hwang, Proc. Natl. Acad. Sci. USA **95**, 11053 (1998).

[3] S. Hwang, A. S. Mukasyan, and A. Varma, Combust. Flame **115**, 354 (1998).

[4] M. W. Beckstead and K. P. McCarty, AIAA J. **20**, 106 (1982).

[5] A. V. Dvoryankin, A. G. Strunina, and A. G. Merzhanov, Comb. Expl. Shock Waves **21**, 421 (1985).

[6] D. P. Mishra, *Experimental Combustion: An Introduction* (CRC Press, Boca Raton, FL, 2014).

[7] N. Kubota and H. Okuhara, Chem. Abstr. **111**, 152 (1989).

[8] N. Kubota, Propell. Explos. **3**, 163 (1978).

[9] Ory Zik and Elisha Moses, Combust. Inst. 2815 (1998).

[10] Ory Zik, Zeev Olami, and Elisha Moses, Phys. Rev. Lett. **81**, 3868 (1998).

[11] Ory Zik and Elisha Moses, Phys. Rev. E **60**, 518 (1999).

[12] A. Varma, A. S. Mukasyan, and S. Hwang, Chem. Eng. Sci. **56**, 1459 (2001).

[13] A. S. Mukasyan, A. S. Rogachev, M. Mercedes, and A. Varma, Chem. Eng. Sci. **59**, 5099 (2004).

[14] A. S. Rogachev and F. Baras, Phys. Rev. E **79**, 026214 (2009).

[15] P. S. Grinchuk and O. S. Rabinovich, Phys. Rev. E **71**, 026116 (2005).

[16] F.-D. Tang, A. J. Higgins, and S. Goroshin, Combust. Theory Model. **13**, 2 319 (2009).

[17] F.-D. Tang, A. J. Higgins, and S. Goroshin, Phys. Rev. E **85**, 036311 (2012).

[18] F. Lam, X. C. Mi, and A. J. Higgins, Phys. Rev. E **96**, 013107 (2017).

[19] S. Goroshin, F.-D. Tang, and A. J. Higgins, Phys. Rev. E **84**, 027301 (2011).

[20] D. B. Spalding, Proc. Roy. Soc. Ser. A **240**, 1220 (1957).

[21] Y. B. Zeldovich, G. I. Barenblatt, V. B. Librovich, and G. M. Makhviladze, *The Mathematical Theory of Combustion and Explosions* (Plenum Press, New York and London, 1985).

[22] N. Provatas, T. Ala-Nissila, M. Grant, K. R. Elder, and L. Piche, Phys. Rev. E **51**, 4232 (1995).

[23] S. A. Rashkovskii, Combust. Expl. Shock Waves **35**, 5 (1999).
[24] S. A. Rashkovskii, Combust. Expl. Shock Waves **38**, 4 (2002).
[25] E. J. Kansa, R. C. Aldredge, and L. Ling, Eng. Anal. Boundary Elem. **33**, 940 (2009).
[26] M. Conti, U. Marini, and B. Marconi, Physica A **312**, 381 (2002).
[27] Z. Lu and Y. Dong, Combust. Theory Model. **15**, 6 795 (2011).
[28] C. Lu and Y. C. Yortsos, Phys. Rev. E **72**, 036201 (2005).
[29] S. N. Menon and G. A. Gottwald, Phys. Rev. E **75**, 016209 (2007).
[30] H. Gotoda, Y. Shinoda, M. Kobayashi, and Y. Okuno, Phys. Rev. E **89**, 022910 (2014).
[31] M. Schiulaz, C. R. Laumann, A. V. Balatsky, and B. Z. Spivak, Phys. Rev. E **97**, 062133 (2018).
[32] S. A. Rashkovskiy, G. M. Kumar, and S. P. Tewari, Combust. Sci. Technol. **182**, 1009 (2010).
[33] N. T. Bharath, S. A. Rashkovskiy, S. P. Tewari, and M. K. Gundawar, Phys. Rev. E **87**, 042804 (2013).
[34] K. L. Klimenok and S. A. Rashkovskiy, Phys. Rev. E **91**, 012805 (2015).
[35] S. A. Rashkovskii and A. Yu. Dolgoborodov, Combust. Explos. Shock Waves **51**, 3 338 (2015).
[36] T. B. Naine and M. K. Gundawar, Indian J. Phys. **91**, 9 (2017).
[37] N. T. Bharath and M. K. Gundawar, Cogent Engineer. **3**, 1185823 (2016).
[38] N. T. Bharat, D. P. Mishra, and M. K. Gundawar, Combust. Sci. Technol. (2019), doi:10.1080/00102202.2019.1565534.
[39] P. L. Krapivsky, S. Redner, and F. Leyvraz, Phys. Rev. Lett. **85**, 4629 (2000).
[40] R. Dickman, Phys. Rev. E **50**, 4404 (1994).
[41] F. M. Izrailev, T. Kottos, A. Politi, S. Ruffo, and G. P. Tsironis, Europhys. Lett. **34**, 6 (1996).
[42] D. P. Mishra, *Fundamentals of Rocket Propulsion* (CRC Press, Boca Raton, FL, 2017).